Crystallization Studies on Linear Aliphatic Polyamides Derived From Naturally Occurring Carbohydrates

C. E. Fernández,[1] M. Bermúdez,[1] A. Alla,[1] M. Mancera,[2] M. G. García-Martín,[2] E. Benito,[2] I. Roffé,[2] J. A. Galbis,[2] S. Muñoz-Guerra[1]

[1]*Departament d'Enginyeria Química, Universitat Politècnica de Catalunya, ETSEIB, Diagonal 647, Barcelona 08028, Spain*
[2]*Departamento de Química Orgánica y Farmacéutica, Facultad de Farmacia, Universidad de Sevilla, Sevilla 41071, Spain*

Received 9 May 2009; accepted 28 July 2009
DOI 10.1002/app.31759
Published online 20 January 2010 in Wiley InterScience (www.interscience.wiley.com).

ABSTRACT: The thermal behavior of three series of sugar-derived polyamides (PA-*n*Su) made from the arabinaric, mannaric and galactaric acids, respectively, and α,ω-alkanediamines containing from 6 to 12 methylene units was investigated by DSC supported by polarizing optical microscopy. Crystallization from the melt under both isothermal and nonisothermal conditions was studied in detail. Melting temperatures of PA-*n*Su were found to decay steadily with the length of the polymethylene segment. Data registered from isothermally crystallized samples were analyzed by the kinetics Avrami approach, which revealed that crystallization initiated by combination of instantaneous and sporadically nucleation. Crystallization half-times indicated that "crystallizability" of PA-*n*Su increases with the number of methylenes in the diamine unit and decreases with the length of the carbohydrate-derived unit. Higher crystallinities were attained for polyamides made of shorter aldaric acids. The relation between thermal data and the configuration of the sugar moiety present in PA-*n*Su was discussed. © 2010 Wiley Periodicals, Inc. J Appl Polym Sci 116: 2515–2525, 2010

Key words: sugar-derived polyamides; carbohydrate-derived polyamides; polyamide crystallization

INTRODUCTION

Polyamides derived from naturally occurring carbohydrates are object of particular attention due to the great interest that polymers from renewable resources are showing nowadays.[1–4] Furthermore, the combination of the excellent thermal and mechanical properties inherent to polyamides with the potential biodegradability that results from the insertion of carbohydrate moieties in the polyamide chain makes sugar-derived polyamides very promising materials for temporary applications in the biomedical field. In the last twenty years, a good amount of work has been done on the synthesis of sugar derived polyamides, in particular on AA-BB-type polyamides. Specifically, linear polyamides derived from aldaric acids have been extensively explored.[5–7] Among them, polyamides made from tartaric acid (threaric acid), which are known in the related literature as poly(tartaramide)s, were the most studied ones[8–10] and their crystal structure and crystallization behavior was investigated in full detail.[11–13] The biodegradability of this family of polyamides has been evidenced in certain cases.[14,15]

Most of linear polyamides made from aldaric acids and alkanediamines are able to crystallize from the melt yielding crystalline materials with melting temperatures between 100 and 250°C. This is a very striking behavior since most of these polyamides are nonstereoregular polymers due to lack of C2 symmetry of the aldaric acid used for synthesis. In fact, only the threo configuration in the tetrose series and the manno and ido configurations in the hexose series have C2 symmetry. However, a fair number of polyamides made from nonsymmetric diacids i.e. arabinaric, xylaric or galactaric, have been reported to be crystalline, a fact that raises serious questions about what is the effect of stereoregularity on crystallinity in polyamides containing sugar derived residues.

The crystalline structure and crystallization behavior of polyamides have been extensively investigated for the last 70 years.[16–18] In fact, a good number of crystallization studies[19–21] have been made to understand the crystallization kinetics of conventional unsubstituted AA-BB and AB-polyamides. Nevertheless, crystallization studies on polyamides containing asymmetric centers in the main chain are very scarce.

Additional Supporting Information may be found in the online version of this article.

Correspondence to: S. Muñoz-Guerra (sebastian.munoz@upc.edu).

Contract grant sponsor: CICYT; contract grant number: MAT2006-13209-C02.

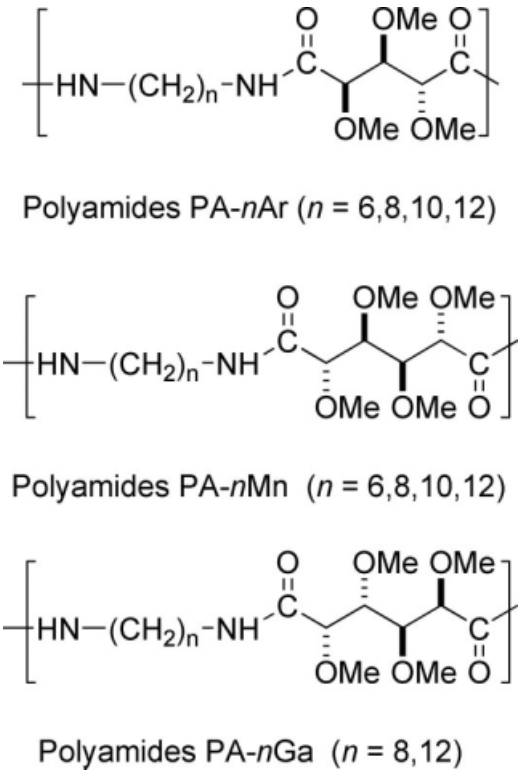

Scheme 1 Chemical structures of PA-*n*Su.

As far as we are aware, the only crystallization study on polyamides containing sugar derived units that has been published is a compared kinetics analysis of the enantiomeric pair of polyamides made of L and D-tartaric acids and hexamethylenediamine.[22] The aim of the present article is to characterize the crystallization behavior of a set of novel polyamides derived from α,ω-alkylene diamines and aldaric acids of five and six carbon atoms with the side hydroxyl groups protected as methyl esters. These polyamides are abbreviated as PA-*n*Su, where *n* is the number of methylenes contained in the diamine unit and Su refers to the configuration of the parent monosaccharide which the aldaric acid comes from. Specifically, polyamides for n = 6, 8, 10, and 12, with the diacid being L-arabinaric (PA-*n*Ar), L-mannaric (PA-*n*Mn) and L-galactaric (PA-*n*Ga) are examined. The chemical structures of these polyamides are depicted in Scheme 1.

The crystallization study has been made under both isothermal and nonisothermal conditions. The information drawn from this study is considered of interest to appraise the potential of these sugar-derived polyamides to be processed by usual melting-crystallization methods. To correlate the "crystallizability" (crystallization rate and attainable crystallinity) with the constitution of PA-*n*Su, the study is covering the detailed analysis of all the members of the three series of PA-*n*Su mentioned earlier, including a good number of experiments with generation of a good number of data. To avoid an excessive presentation of figures, the report is illustrated by using graphical data only for PA-12Ar and PA-12Mn, which have been selected as adequate representative examples of the whole collection of PA-*n*Su; similar data for all other polyamides are afforded in the Supporting Information which has been attached to the main text.

EXPERIMENTAL

The synthesis and characterization of the series PA-*n*Ar, PA-*n*Mn, and PA-*n*Ga have been reported in detail elsewhere.[5] They were prepared by polycondensation in solution of the aldaric acids and the corresponding α,ω-alkylenediamines containing even numbers of methylenes from 6 to 12. The main features of these polyamides with relevance to the present study are compared in Table I.

TABLE I
Molecular Weights and Thermal Data of PA-*n*Su

PA-*n*Su	M_w[a] (g mol^{-1})	M_n[a] (g mol^{-1})	T_m[b] (°C)	ΔH_m[b] (J g^{-1})	T_g[c] (°C)	T_d[d] (°C)	T_m^0[e] (°C)
PA-6Ar	41,600	29,400	226	50	95	**395**/460	239
PA-8Ar	86,600	53,400	210	46	80	**395**/463	210
PA-10Ar	136,000	74,600	200	34	77	**404**/477	206
PA-12Ar	115,000	70,300	192	47	70	398/**474**	200
PA-6Mn	42,300	30,800	188	39	87	**406**/475	200
PA-8Mn	78,400	57,200	173	26	76	**400**/454	192
PA-10Mn	71,000	45,800	165	35	57	**404**/475	178
PA-12Mn	158,100	124,000	152	29	70	**403**/472	161
PA-8Ga	55,300	38,100	213	32	83	396/456	229
PA-12Ga	107,700	75,400	203	32	79	432/450	219

[a] Weight-average and number-average molecular weights of samples coming from synthesis.
[b] Melting temperature and enthalpy of samples coming from synthesis determined at the heating rate of 10°C min^{-1}.
[c] Glass transitions determined at a heating rate of 20°C min^{-1} from quenched samples.
[d] Decomposition temperature measured as the peak of the derivatives curves, main peak in bold.
[e] Equilibrium melting temperatures determined according to Hoffman and Weeks.[23]

Differential scanning calorimetry (DSC) measurements were carried out on a Perkin–Elmer calorimeter Pyris 1 calibrated with indium using either powder samples coming directly from synthesis or films prepared by casting. DSC data were obtained from 4 to 6 mg samples at a heating rate of 10°C min^{-1} under a nitrogen flow of 20 mL min^{-1}. Glass transition temperatures were measured at a heating rate of 20°C min^{-1} from melt-quenched samples. Isothermal crystallizations were accomplished by heating the samples for 5 min above T_m at temperatures, to erase all previous thermal history and then quenched at the nominal rate of 80°C min^{-1} to the chosen crystallization temperature T_c. The samples were held at T_c for the time necessary to develop the maximum detectable crystallinity and then they were heated from T_c to above melting to record their fusion behavior. The melting peak temperatures observed after isothermal crystallization were used to calculate the equilibrium melting temperatures of PA-*n*Su. nonisothermal crystallization experiments were recorded at cooling rates of 2.5, 5, 10, 20, and 40°C min^{-1}. As a representative example, the scanning cycle applied for PA-6Mn was as follows: The sample was heated to 230°C and held at this temperature for 5 min, then cooled down at 2.5°C min^{-1} to 0°C, held at this temperature for 1 minute, and finally heated again to 230°C at 10°C min^{-1}.

Polarized optical microscopy (POM) was performed using an Olympus BX51 microscope with a digital camera attached. Cast films were obtained from both chloroform and formic acid at room temperature. Films crystallized from the melt were prepared by heating the polymer between two microscope cover slips at a temperature above T_m for 5 min and then cooling quickly to the crystallization temperature. A hot-stage Linkam THMS 600 provided with a N_2 cooling system was used for this study.

RESULTS AND DISCUSSION

Nonisothermal crystallization

Firstly, the nonisothermal crystallization behavior of PA-*n*Su was examined. The traces registered at different cooling rates and the subsequent heating traces obtained for the representative polyamides PA-12Ar and PA-12Mn are compared in Figure 1. A single exothermic peak was observed at cooling for

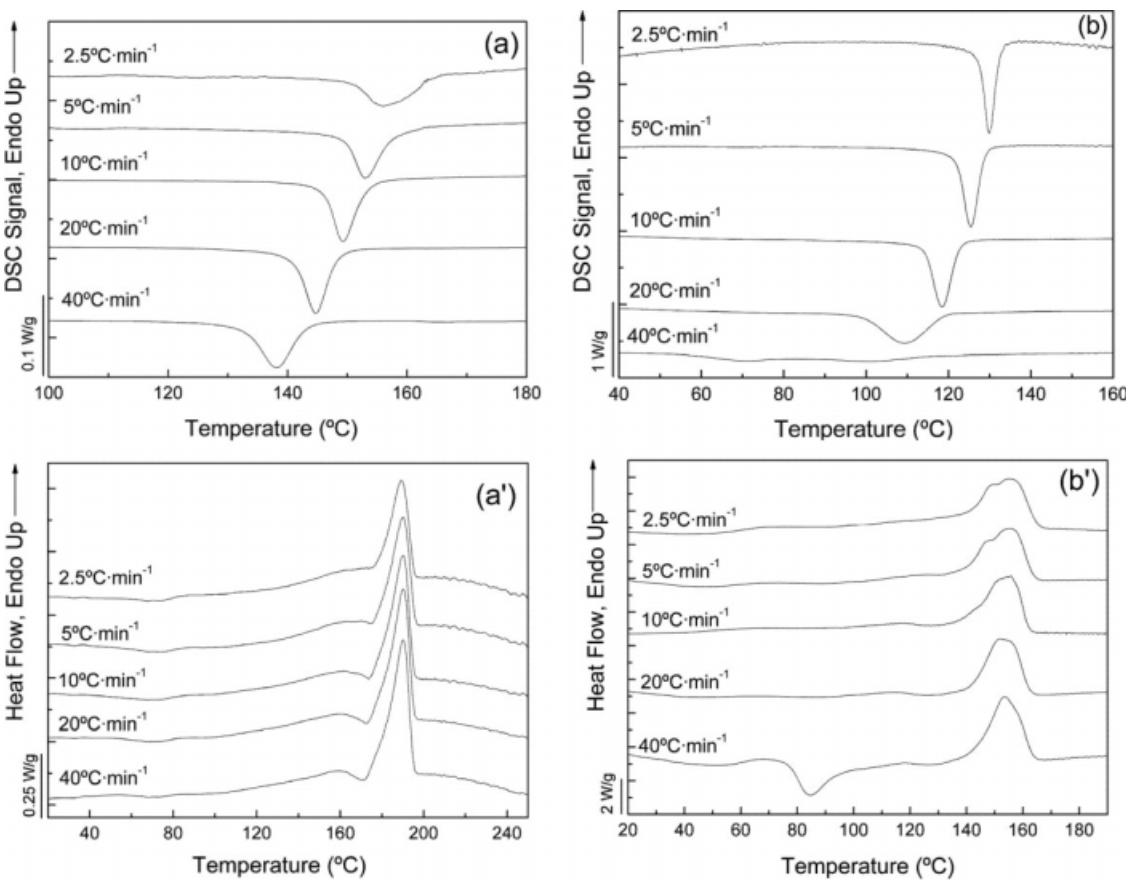

Figure 1 DSC cooling traces from PA-12Ar (a) and PA-12Mn (b) registered at the indicated cooling rates and the heating traces from the corresponding crystallized samples (a′ and b′).

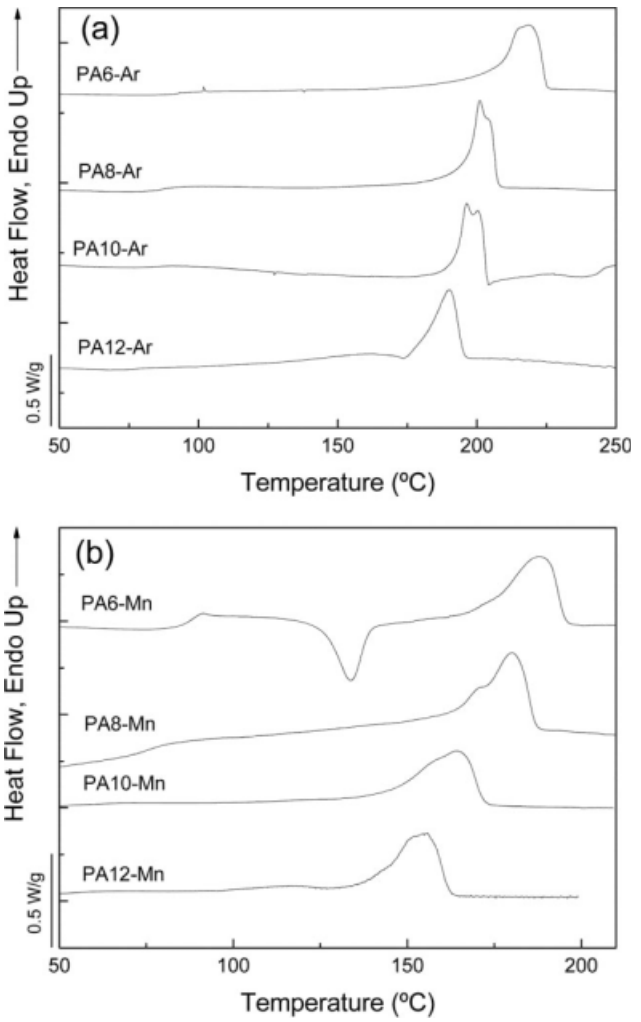

Figure 2 Comparative heating traces of PA-*n*Ar (a) and PA-*n*Mn (b) crystallized from the melt at 10°C min^{-1}.

the two polyamides and their corresponding heating traces showed some significant differences; PA12-Ar showed a sharp single melting peak preceded by a cold crystallization exothermal while PA12-Mn showed a broad melting peak that became split for samples that were crystallized at low cooling rates. In both cases, the crystallization temperature decreased and the melting temperature increased slightly as the cooling rate applied for crystallization decreased. The DSC traces recorded for all the others PA-*n*Su showed features similar to one of these two. It was also noticed for all the polyamides showing double melting, that the higher temperature component was not sensitive to the cooling rate, i.e. no significant change in either temperature or enthalpy was observed. Such behavior is consistent with the occurrence of a reorganization process taking place at heating, in which the polymer melts at low temperature and immediately recrystallizes to remelt in the second peak. This type of processes consisting of partial melting followed by recrystallization and melting has been reported for a good number of polyesters and polyamides.[20,21,23]

The influence of the length of the polymethylene segment on the melting behavior of non-isothermally crystallized PA-*n*Su is illustrated in Figure 2, where the DSC heating traces recorded for the series PA-*n*Ar and PA-*n*Mn are compared. As it is clearly evidenced in the plot constructed in Figure 3 using these melting data, a decrease in the melting temperature takes place as the numbers of methylenes contained in the repeating unit of the polyamide increases following a nearly linear trend. Such behavior is fully reasonable since the density of hydrogen bonds decreases steadily with the length of the polymethylene segment. A similar result was obtained by plotting T_c against n. On the contrary, melting and crystallization enthalpies did not show any apparent dependence on n.

Isothermal crystallization

Thin films of PA-*n*Su crystallized from the melt or by casting from either chloroform or formic acid produced more or less well-delineated spherulitic textures depending on the polyamide that is crystallized and on crystallization conditions. Large spherulites displaying well defined Maltese cross and clearly separated extinction bands were readily obtained for all PA-*n*Su by casting whereas samples crystallized from the melt displayed a diversity of appearances going from coarse granular textures to well delineated impinging spherulites. A selection of illustrative pictures for the PA-*n*Mn and PA-*n*Ga series are depicted in Figure 4 and an additional collection covering all the studied series is afforded in the Supporting Information. What becomes apparent

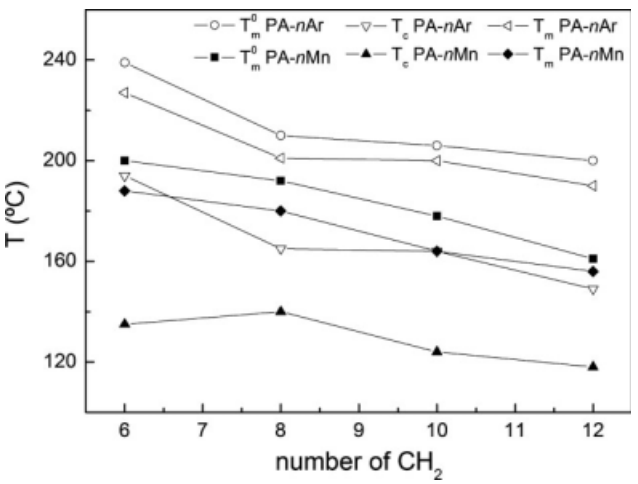

Figure 3 Crystallization or melting temperature (a) and enthalpy (b) vs the number of CH_2 in the repeating unit of PA-*n*Su. (T_c, Crystallization temperature; T_m, Melting temperature of samples crystallized from the melt at 10°C min^{-1}; T^0_m, Equilibrium melting temperature).

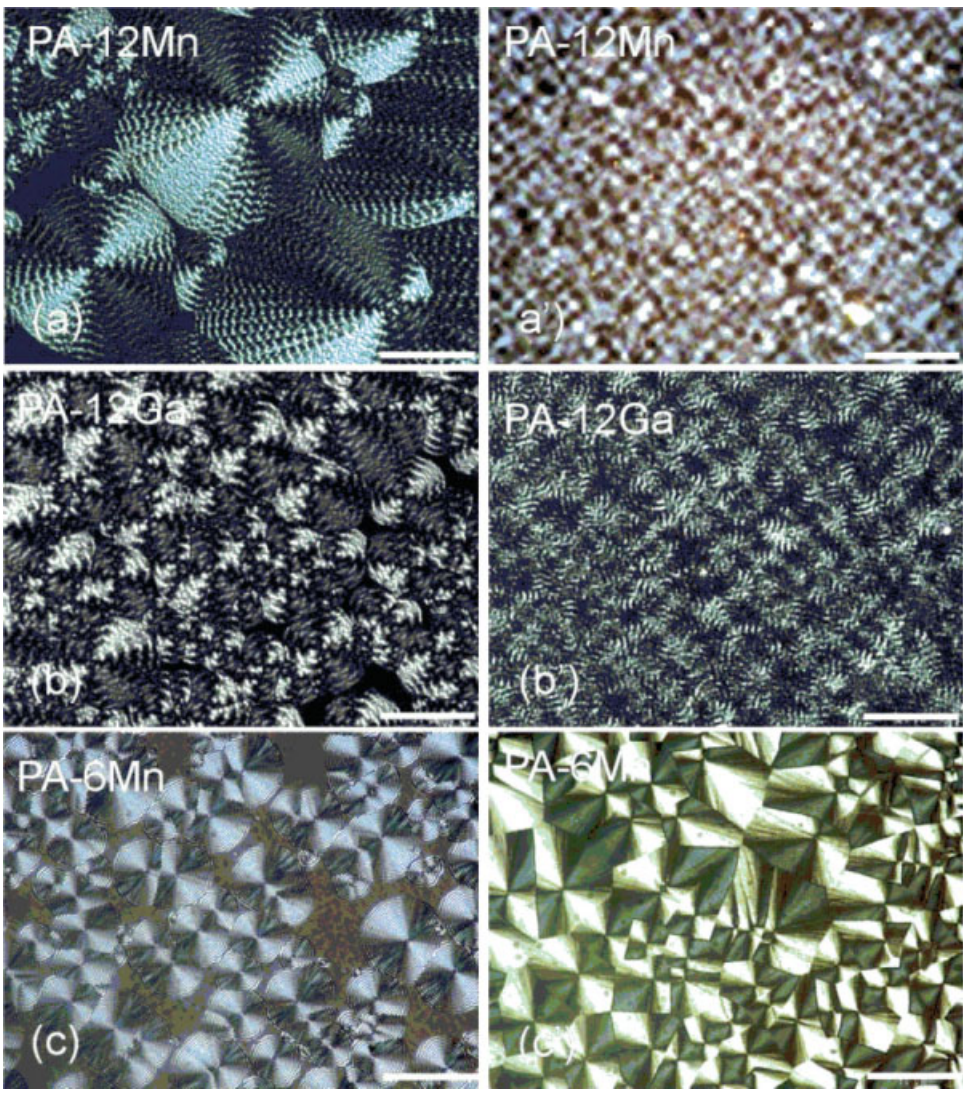

Figure 4 Cross polarized light micrographs of thin films of PA-*n*Su prepared by casting from formic acid (a, b, and c) and by cooling from the melt (a′, b′, c′). The bar represents 5 μm. [Color figure can be viewed in the online issue, which is available at www.interscience.wiley.com.]

from these microscopical observations is the occurrence of overcrowded nucleation in the crystallization from the melt which prevents spherulites to attain large dimensions, at least the dimensions required for a satisfactory observation under the polarizing microscope. This fact will also prevent the analysis of the crystallization kinetics on individual spherulites.

The isothermal crystallization of PA-*n*Su at different temperatures was studied by DSC and data obtained were analyzed using the Avrami approach[24–26] according to the following equation:[24]

$$1 - V_c\,(t - t_0) = e^{-k(t-t_0)^{n^A}} \qquad (1)$$

where V_c is the relative volume fraction of crystallized material normalized by the maximum crystallization enthalpy, t_0 is the induction time, i.e. the time elapsed before any vestige of crystallinity was detected, t is crystallization time, and k and n^A are the Avrami parameters related with the global crystallization rate and the polymer nucleation and growing dimensionality, respectively.[27]

The crystallization isotherms for PA-12Ar and PA-12Mn obtained at 135 and 170°C, respectively, and expressed as the change in volume fraction of amorphous material with crystallization time, along with the double logarithmic plots of such data, are shown in Figure 5. These data were adjusted to the Avrami equation and found to fit well –correlation coefficients were found to be greater than 0.99 in all cases– provided that conversion was confined to the interval of 3–30% of relative crystallinity, i.e. within the primary crystallization range. Similar

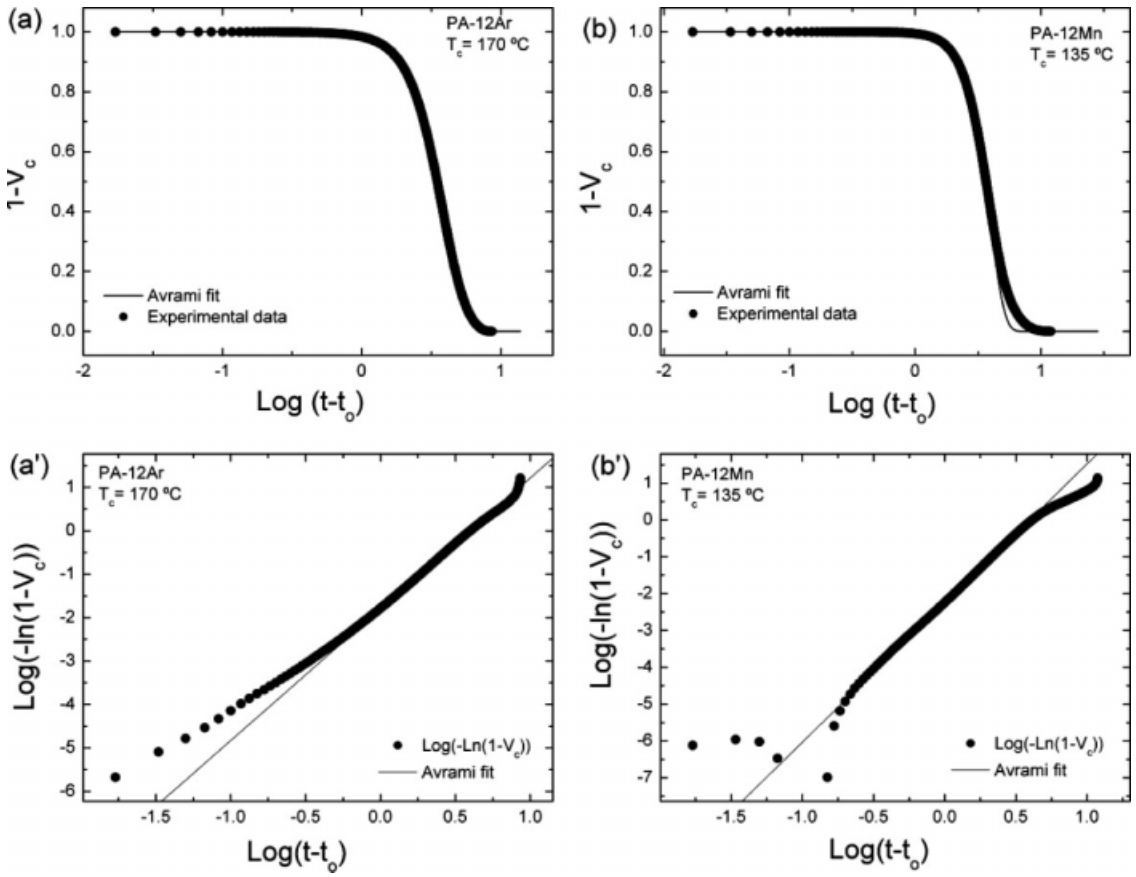

Figure 5 Isothermal crystallization data for PA-12Ar (a and a′) and PA-12Mn (b and b′) at the indicated crystallization temperatures. The best Avrami fit is superposed to experimental data in the four plots.

experimental data displaying a similar degree of fitness to the Avrami equation were obtained for all the other PA-*n*Su. This information is additionally supplied in the Supporting Information accompanying this article. The experimental isothermal crystallization curve registered by DSC was simulated using the Avrami's equation by means of the procedure reported by Lorenzo et al.[28] Figure 6 shows these fits for PA-12Ar and PA-12Mn at the indicated temperatures; it can be seen that coincidence is excellent up to near 30% of conversion indicating that primary crystallization is the only process operating within such ranges of time. At longer crystallization times the calculated trace deviates more or less from the experimental data as it should be expected from the occurrence of impeded secondary crystallization that is known to take place usually in polymer crystallization at high conversions.

Numerical data extracted from such plots are compared in Tables II–IV for the three series PA-*n*Ar, PA-*n*Mn and PA-*n*Ga and for all the crystallization temperatures that were assayed. The Avrami constant k is observed to decrease with crystallization temperature for every studied polyamide whereas the Avrami exponent values were found to oscillate between 2.5 and 4 for most of cases (more than 80%). Such values are indicative that spherulites could be either instantaneously or sporadically nucleated and that crystallization recedes as T_c increases although the growth mechanism does not vary in a steady manner. Other crystallization data contained in Tables II–IV were analyzed to relate the "crystallizability" of PA-*n*Su with the constitution of the polyamide regarding the influence of both the diamine and the aldaric units on crystallization rate. Unfortunately, the temperature range in which enthalpy is measurable and therefore crystallization may be perceived, varies largely from one polyamide to another so that a comparison embracing the whole family of polyamides for a same supercooling (ΔT) is not feasible. Nevertheless, sufficient data were collected to reach meaningful conclusions in this regards. For a straightforward interpretation of such data, the inverse of crystallization half-times against the applied supercooling were plotted in Figure 7 and compared for PA-*n*Su differing either in n or in the aldaric constitution. The conclusions drawn from these plots are the following:

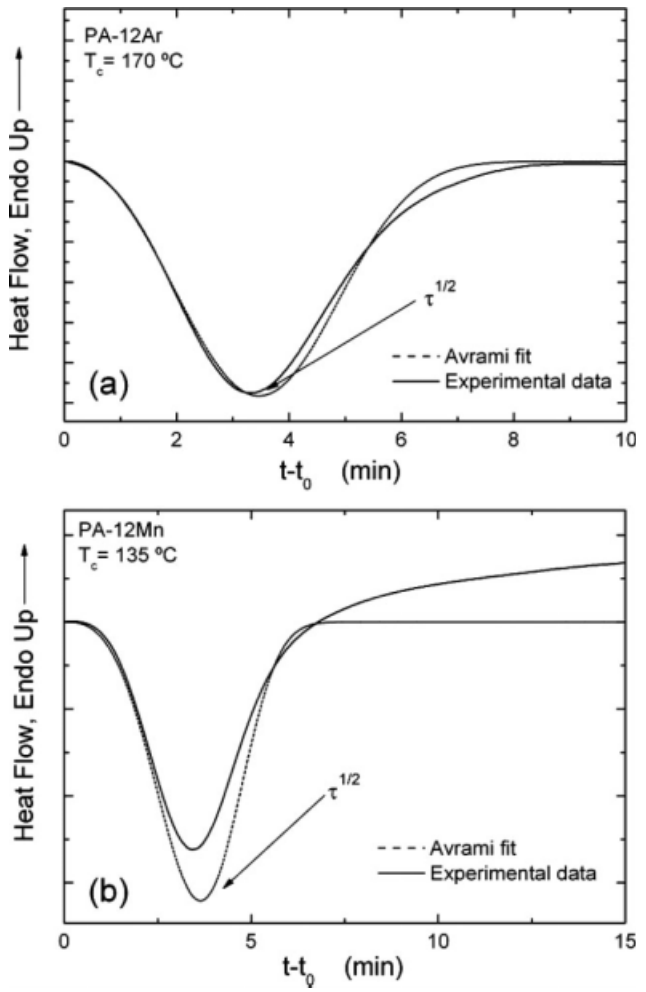

Figure 6 DSC traces of isothermal crystallization of PA-12Ar (a) PA-12Mn (b) at the indicated crystallization temperatures with superimposed Avrami fits obtained by applying the procedure of Lorenzo et al.[28]

a. As it is clearly seen for all the plots represented in Figure 7 without exception, crystallization half-time $t_{1/2}$ increases with the degree of supercooling at which crystallization was set to occur, i.e. the crystallization rate decreases with crystallization temperature. It is a consistent result that indicates that experiments were confined in a temperature range in which molecular transport was the factor determining the crystallization rate.
b. Comparison of $1/t_{1/2}$vs ΔT plots for PA-*n*Su containing the same sugar unit but differing in *n* [Fig. 7(a,b)] reveals that for a given supercooling, $t_{1/2}$ decreases as *n* increases. This means that long diamine units favor crystallization rate of PA-*n*Su. This is a behavior shared by polyamides in general that is well account by considering the diluting effect of the alkylene segment on hydrogen-bonds.
c. Comparison of $1/t_{1/2}$vs ΔT plots for PA-*n*Su containing the same diamine unit but differing in the diacid unit [Fig. 7(c)] reveals that for a given supercooling, $t_{1/2}$ decreases as moving from 8Ar to 8Mn with 8Ga displaying an intermediate value along the whole range of ΔT examined. Similar results were obtained by comparing PA-*n*Su for other *n* values. It seems that crystallization rate is favored by shorter sugar units but disfavoured by the symmetric manno configuration present in the polyamide PA-8Mn. This conclusion has been additionally supported by extending the comparison to the analogous polyamide derived from tartaric acid PA-6Th previously published by us.[22] Experimental data available for the isothermal crystallization of this polyamide was analyzed to define its equilibrium temperature and hence the supercooling ranges used for crystallization. These data allows comparing directly the crystallization rate for PA-6Th, PA-6Ar, and PA6-Mn within the same range of ΔT. The $t_{1/2}$ for these three polyamides are plotted in Figure 8(a) to bring out how the crystallization rate decreases as the size of the sugar moiety increases.

The accumulated enthalpy value measured at the end of the isothermal crystallization experiment affords a relative estimation of the degree of crystallinity reached in each case. A comparison of the enthalpy values given in Tables II–IV reveals that the crystal fraction generated upon crystallization tends to decrease with the amount of supercooling that is applied. It is additionally observed that ΔH decreases as the size of the sugar residue increases; this observation is sustained by taking into account the values reported for PA-6Th.[22] On the contrary, the variation of ΔH with *n* does not change significantly within each PA-*n*Su series indicating that the crystallinity attainable is scarcely dependent on the length of the diamine unit.

The DSC heating traces recorded from samples of PA-12Ar and PA-12Mn that were isothermally crystallized are shown in Figure 9. In the three cases a complex melting endotherm containing two or three peaks that displaces towards higher temperatures with crystallization temperature, is observed; the same behavior is shared by all others isothermally crystallized PA-*n*Su. The presence of multiple melting peaks is a common observation in the DSC traces of polyamides crystallized under isothermal conditions[23,29] and it is comparable to the double melting peak observed for the non-isothermally crystallized samples described earlier. In both cases, the lower temperature shoulder (T_m^1) accompanying the main melting peak (T_m^2) should be attributed to the

TABLE II
Isothermal Crystallization Parameters for PA-*n*Ar at Different Temperatures

PA-6Ar					
T_c (°C)[a]	203	205	207	209	211
n^{Ab}	1.9	2.5	2.8	2.4	2.7
k (min^{-n})[b]	1.03	0.54	0.22	0.044	0.0033
$\tau^{1/2}$ (min)[c]	0.98	1.35	1.73	3.41	8.56
$\tau^{1/2}$ (min)[d]	0.81	1.10	1.50	3.14	7.48
t_0 (min)[e]	0.4	0.41	0.63	1.4	2.08
ΔH_c (J g^{-1})[f]	16	19	15	11	20
R^2	0.9993	0.9992	0.9995	0.9998	0.9979
V_c[g]	3-20	3-20	3-20	3-20	3-20
PA-8Ar					
T_c (°C)[a]	170	175	180	182.5	185
n^{Ab}	2.6	3.3	3.1	2.6	2.9
k (min^{-n})[b]	7.08	0.42	0.03	0.023	0.004
$\tau^{1/2}$ (min)[c]	0.40	1.11	2.70	3.63	5.63
$\tau^{1/2}$ (min)[d]	0.40	1.15	2.74	3.68	5.69
t_0 (min)[e]	0.30	0.36	0.61	1.31	1.43
ΔH_c (J g^{-1})[f]	36	37	33	31	29
R^2	0.9992	0.9990	0.9999	0.9999	1
V_c[g]	3-20	3-20	3-20	3-20	3-20
PA-10Ar					
T_c (°C)[a]	175	177.5	180	182.5	185
n^{Ab}	3.1	3.4	3.1	3.0	2.5
k (min^{-n})[b]	0.23	0.02	0.007	0.0011	0.0010
$\tau^{1/2}$ (min)[c]	1.43	2.70	4.23	8.28	13.81
$\tau^{1/2}$ (min)[d]	1.43	2.63	4.16	8.12	13.55
t_0 (min)[e]	0.45	0.55	1.08	2.05	7.7
ΔH_c (J g^{-1})[f]	33	32	32	32	24
R^2	0.9999	0.9999	1	1	0.9999
V_c[g]	3-20	3-20	3-20	3-20	3-20
PA-12Ar					
T_c(°C)[a]	160	162.5	165	167.5	170
n^{Ab}	2.7	3.0	2.8	3.4	3.0
k (min^{-n})[b]	0.38	0.13	0.12	0.023	0.015
$\tau^{1/2}$ (min)[c]	1.21	1.73	1.83	2.76	3.5
$\tau^{1/2}$ (min)[d]	1.24	1.74	1.85	2.70	3.50
t_0 (min)[e]	0.4	0.4	0.63	0.58	1.15
ΔH_c (J g^{-1})[f]	25	25	25	27	23
R^2	0.9993	0.9996	0.9998	1	0.9999
V_c[g]	3-20	3-20	3-20	3-20	3-20

[a] Crystallization temperature.
[b] Parameters of Avrami equation.
[c] Crystallization half-time determined experimentally.
[d] Crystallization half-time calculated by Avrami as $(Ln2/k)^{1/n}$.
[e] Crystallization onset time.
[f] Crystallization enthalpy.
[g] Range of crystalline volume fraction taken for kinetics calculations.

melting of a population of defective crystallites formed on the boundary of the larger ones at the later stage of the isothermal crystallization (secondary crystallization).[29] The temperatures measured for the higher melting peak were used for determining graphically the equilibrium melting temperatures of PA-*n*Su according to the procedure of Hoffman and Weeks.[30] The plot of T_m vs T_c should result in a straight line that upon extrapolation will intersect with the $T_m = T_c$ line at the equilibrium temperature. These plots are depicted in Figure 10 for PA-12Ar and PA-12Mn. The same procedure was applied to determine T^0_m for all the other PA-*n*Su studied in this work; the values obtained for the whole family are given in Table I and their corresponding graphical data are provided in the

TABLE III
Isothermal Crystallization Parameters for PA-*n*Mn at Different Temperatures

PA-6Mn					
T_c (°C)[a]	155	157.5	160	162.5	165
n^{Ab}	2.7	2.4	2.4	2.8	2.6
k (min^{-n})[b]	0.047	0.052	0.032	0.0092	0.011
$\tau^{1/2}$ (min)[c]	2.70	2.88	3.53	4.76	5.10
$\tau^{1/2}$ (min)[d]	2.68	2.89	3.51	4.71	4.97
t_0 (min)[e]	0.75	1.13	1.23	1.08	1.83
ΔH_c (J g^{-1})[f]	34	31	29	31	20
R^2	0.9999	0.9999	1	0.9999	0.9998
V_c[g]	3-30	3-30	3-30	3-30	3-30
PA-8Mn					
T_c (°C)[a]	160		162.5		165
n^{Ab}	2.9		2.9		2.3
k (min^{-n})[b]	9.98×10^{-04}		7.74×10^{-04}		0.0011
$\tau^{1/2}$ (min)[c]	9.15		10.36		15.96
$\tau^{1/2}$ (min)[d]	8.13		10.60		15.92
t_0 (min)[e]	2		6.78		13.23
ΔH_c (J g^{-1})[f]	24		22		15
R^2	0.9963		0.9997		0.9997
V_c[g]	3-15		3-20		3-20
PA-10Mn					
T_c (°C)[a]	140	142.5		145	147.5
n^{Ab}	3.2	3.2		3.1	2.7
k (min^{-n})[b]	0.029	0.0095		0.0037	0.0011
$\tau^{1/2}$ (min)[c]	2.75	3.91		5.86	11.20
$\tau^{1/2}$ (min)[d]	2.66	3.74		5.48	10.38
t_0 (min)[e]	0.53	0.8		1.28	2.4
ΔH_c (J g^{-1})[f]	31	30		26	23
R^2	0.9999	0.9999		0.9994	0.9991
V_c[g]	3-20	3-20		3-20	3-20
PA-12Mn					
T_c (°C)[a]	130	132.5	135	137.5	140
n^{Ab}	3.7	4.0	3.3	3.4	3.5
k (min^{-n})[b]	0.12	0.022	0.0135	0.0015	$5{\cdot}16 \times 10^{-04}$
$\tau^{1/2}$ (min)[c]	1.63	2.45	3.33	5.86	7.70
$\tau^{1/2}$ (min)[d]	1.60	2.36	3.30	5.89	7.71
t_0 (min)[e]	1.03	1.11	1.98	2.95	4.01
ΔH_c (J g^{-1})[f]	26	26	26	29	26
R^2	0.9998	0.9999	0.9999	0.9999	0.9999
V_c[g]	3-20	3-20	3-20	3-20	2-30

[a] Crystallization temperature.
[b] Parameters of Avrami equation.
[c] Crystallization half-time determined experimentally.
[d] Crystallization half-time calculated by Avrami as $(Ln2/k)^{1/n}$.
[e] Crystallization onset time.
[f] Crystallization enthalpy.
[g] Range of crystalline volume fraction taken for kinetics calculations.

TABLE IV
Isothermal Crystallization Parameters for PA-*n*Ga at Different Temperatures

PA-8Ga				
T_c (°C)[a]	195	197.5	202.5	205
n[b]	3.3	3.0	2.8	2.4
k (min^{-n})[b]	0.07	0.027	0.001	0.001
$\tau^{1/2}$ (min)[c]	2.05	3.03	8.55	13.13
$\tau^{1/2}$ (min)[d]	1.93	2.97	8.36	13.03
t_0 (min)[e]	0.96	1.75	6.9	15.43
ΔH_c (J g^{-1})[f]	25	22	15	12
R^2	0.9999	0.9999	0.9999	0.9998
V_c[g]	3-20	3-20	3-20	3-20
PA12-Ga				
T_c (°C)[a]	180	182.5	185	187.5
n[b]	3.2	3.3	2.9	2.9
k (min^{-n})[b]	0.36	0.0094	0.001	1.89×10^{-04}
$\tau^{1/2}$ (min)[c]	1.33	3.86	8.36	18.66
$\tau^{1/2}$ (min)[d]	1.22	3.63	8.10	17.06
t_0 (min)[e]	0.56	1.25	4.8	12.68
ΔH_c (J g^{-1})[f]	8	19	12	9
R^2	0.9998	0.9995	0.9999	0.9994
V_c[g]	3-20	3-20	3-20	3-20

[a] Crystallization temperature.
[b] Parameters of Avrami equation.
[c] Crystallization half-time determined experimentally.
[d] Crystallization half-time calculated by Avrami as $(\text{Ln}2/k)^{1/n}$.
[e] Crystallization onset time.
[f] Crystallization enthalpy.
[g] Range of crystalline volume fraction taken for kinetics calculations.

Supporting Information. In polyamides, the value of T_m^0 is closely related to the density of amide groups along the polymer chain so that higher T_m^0 values are usually observed for higher amide densities.[29] The values obtained for PA-*n*Su are in full concordance with this general pattern of behavior. It has to be noted that temperatures recorded for the lower melting peak are not suitable for the determination of T_m^0 since the trend line remains nearly parallel to the $T_m = T_c$ line; this supports the interpretation of such low temperature peak as due to the melting of material crystallized out of thermal control.

CONCLUSIONS

The crystallization of three series of sugar-derived polyamides PA-*n*Ar, PA-*n*Mn, and PA-*n*Ga was investigated under isothermal and nonisothermal conditions. Films of these polyamides crystallized by casting or from the melt displayed banded or fibrillar spherulitic textures. Heating of both isothermally and non-isothermally crystallized samples of PA-*n*Su displayed complex melting peaks as a result of the presence of multiple crystallite populations differing in size and/or the occurrence of melting-recrystallization-melting process. As a general rule, the melting temperatures of PA-*n*Su decreased with the increasing number of methylene units in the diamine segment. Avrami parameters resulting from the analysis of isothermal crystallization data indicated

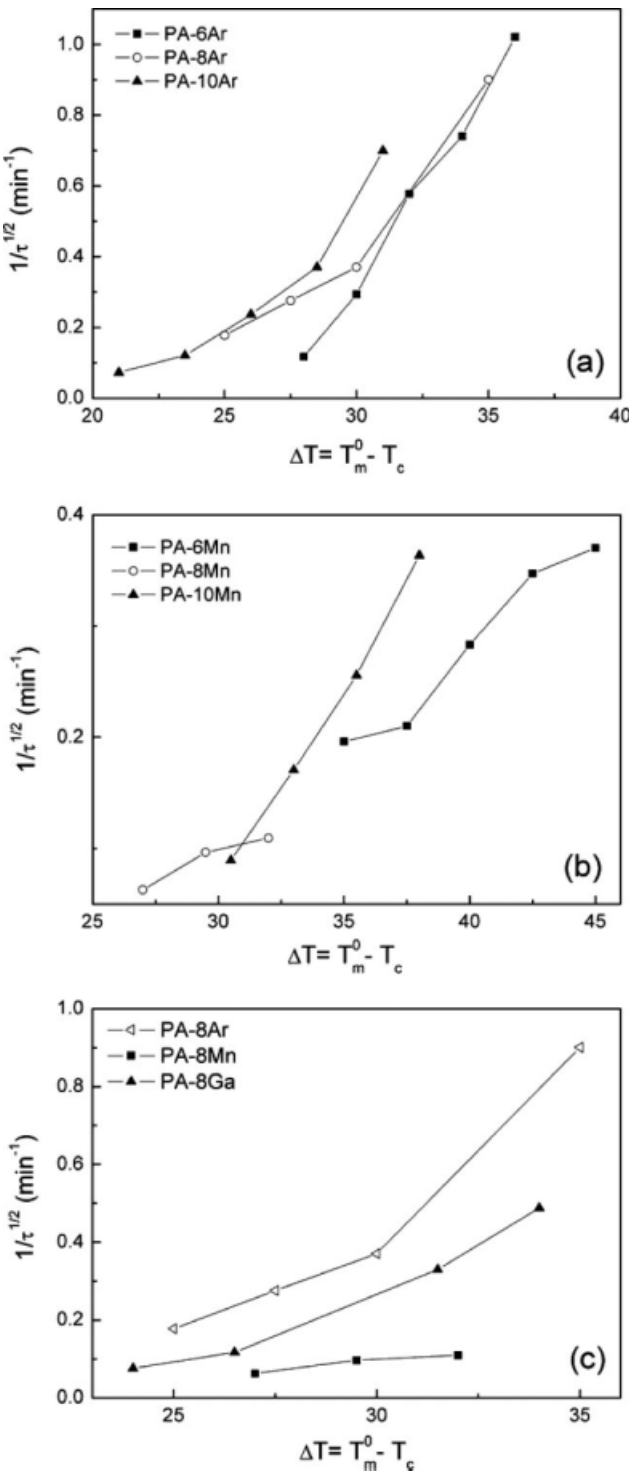

Figure 7 Inverse of the experimental crystallization half-time $1/t_{1/2}$ vs $\Delta T = T_m^0 - T_c$ for the indicated PA-*n*Su.

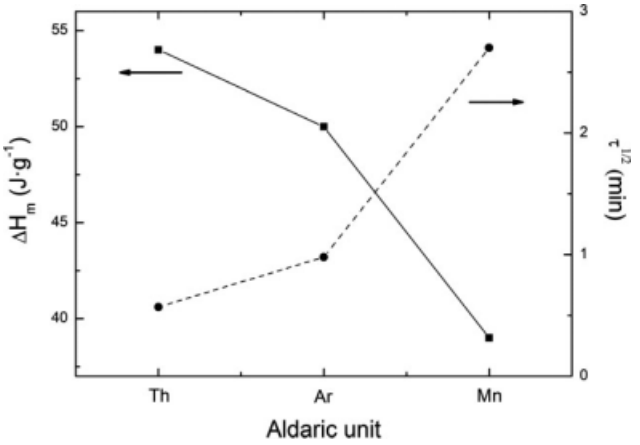

Figure 8 Variation of crystallization enthalpy and crystallization half-time $t_{1/2}$ of PA-*n*Su as a function of the aldaric unit containing in the chain.

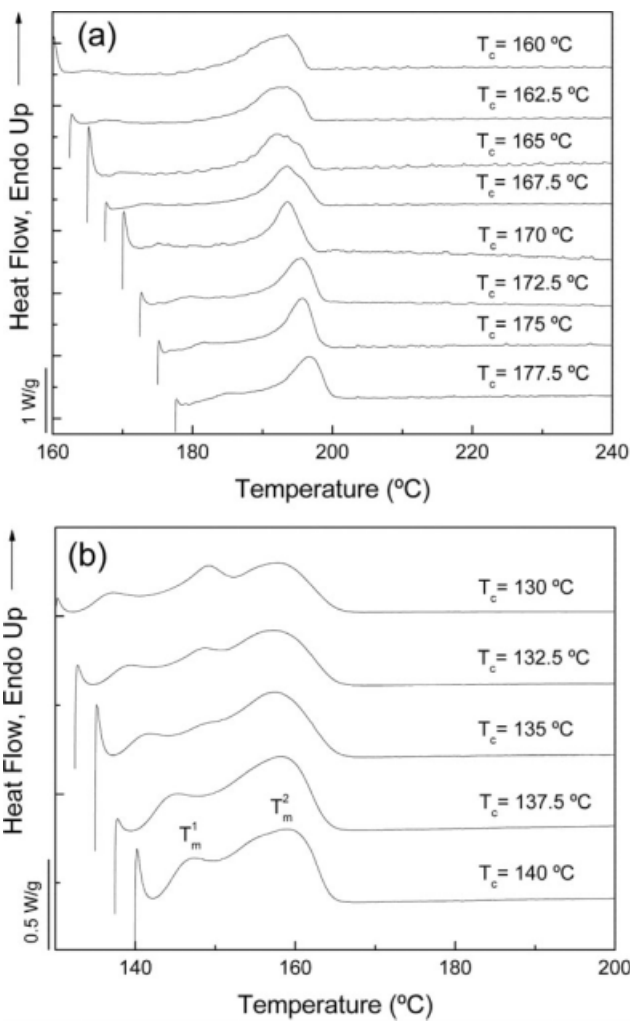

Figure 9 DSC heating traces of samples of PA-12Ar (a) and PA-12Mn (b) isothermally crystallized at the indicated temperatures.

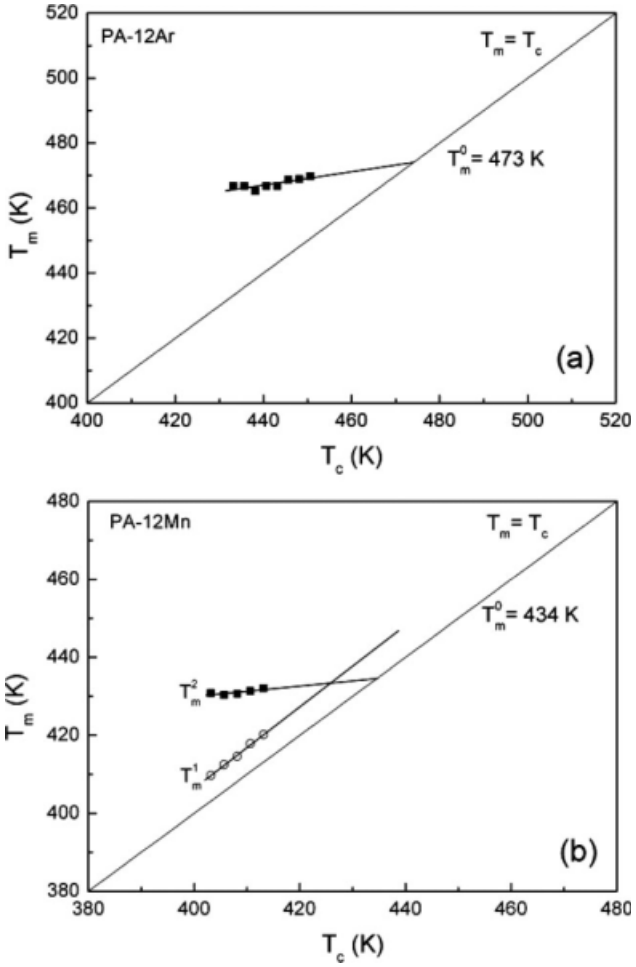

Figure 10 Determination of the equilibrium melting temperature T_m^0 for PA-12Ar (a) and PA-12Mn (b).

that the crystallization process is initiated by a combination of instantaneous and sporadically nucleation. As a general rule, the crystallization rates for each studied polyamide were observed to decrease with the degree of supercooling. The "crystallizability" of PA-*n*Su was found to be largely determined by the constitution of the polyamide. Thus the crystallization rate was found to be dependent on both the length of the polymethylene segment and the chemical structure of the sugar derived moiety. On the contrary, the amount of crystallinity attainable by isothermal crystallization appeared to be only affected by the size of the sugar unit.

The authors thank AGAUR for the Ph.D. grant awarded to Carlos E. Fernández. They thank Prof. A. Muller (Universidad Simon Bolívar, Caracas, Venezuela) for their useful suggestions and enriching discussions.

References

1. Okada, M. Prog Polym Sci 2002, 27, 87.
2. Thiem, J.; Bachmann, F. Trends Polym Sci 1994, 2, 425.
3. Golcanves, K. E.; Mungara, P. M. Trends Polym Sci 1996, 4, 25.

4. Varela, O.; Orgueira, H. A. Adv Carbohyd Chem Biochem 1999, 55, 137.
5. Mancera, M.; Roffé, I.; Bermúdez, M.; Allá, A.; Muñoz-Guerra, S.; Galbis, J. A. Macromolecules 2004, 37, 2779.
6. García-Martín, M.; Benito, E.; Ruiz, R.; Alla, A.; Muñoz-Guerra, S.; Galbis, J. A. Macromolecules 2004, 37, 5550.
7. Bou, J.; Rodríguez-Galán, A.; Muñoz-Guerra, S. Encyclopedia of Polymeric Materials; Salomone, J. C., Ed.; CRC Press: Boca Ratón, 1996; pp 561–569.
8. Rodríguez-Galán, A.; Bou, J. J.; Muñoz-Guerra, S. J Polym Sci Part A: Polym Chem 1992, 30, 713.
9. Bou, J. J.; Rodríguez-Galán, A.; Muñoz-Guerra, S. Macromolecules 1993, 26, 5664.
10. Bou, J. J.; Iribarren, I.; Martínez De Ilarduya, A.; Muñoz-Guerra, S. J Polym Sci Part A: Polym Chem 1999, 37, 983.
11. Regaño, C.; Martínez De Ilarduya, A.; Iribarren, I.; Rodríguez-Galán, A.; Galbis, J. A.; Muñoz-Guerra, S. Macromolecules 1996, 29, 8404.
12. Iribarren, I.; Alemán, C.; Regaño, C.; Martínez De Ilarduya, A.; Bou, J. J.; Muñoz-Guerra, S. Macromolecules 1996, 29, 8413.
13. Iribarren, J. I.; Martínez De Ilarduya, A.; Alemán, C.; Oraison, J. M.; Rodríguez-Galán, A.; Muñoz-Guerra, S. Polymer 2000, 41, 4869.
14. Ruíz-Donaire, P.; Bou, J. J.; Muñoz-Guerra, S.; Rodríguez-Galán, A. J Appl Polym Sci 1995, 58, 41.
15. Marqués, M. S.; Regaño, C.; Nyugen, J.; Aidanpa, L.; Muñoz-Guerra, S. Polymer 2000, 41, 2765.
16. Bunn, C. W.; Garner, E. V. Proc Roy Soc 1947, 189, 39.
17. Murthy, M. S. J Polym Sci Part B: Polym Phys 2006, 44, 1763.
18. Aharoni, S. M. In *n*-Nylons: Their Synthesis, Structure and Properties; Wiley: New York, 1997.
19. Dilorenzo, M. L.; Silvestre, C. Prog Polym Sci 1999, 24, 917.
20. Wunderlich, B. In Thermal Analysis of Polymeric Materials; Springer: Berlin Heidelberg, 2005.
21. Mathot, V. In Calorimetry and Thermal Analysis of Polymers; Hanser Publishers: New York, 1994.
22. Marín, R.; Alla, A.; Muñoz-Guerra, S. Macromol Rapid Commun 2006, 27, 1955.
23. Ren, M.; Mo, Z.; Chen, Q.; Song, J.; Wang, S.; Zhang, H.; Zhao, Q. Polymer 2004, 45, 3511.
24. Avrami, M. Chem Phys 1939, 7, 1103.
25. Avrami, M. Chem Phys 1940, 8, 212.
26. Avrami, M. Chem Phys 1941, 9, 177.
27. Gedde, U. W. In Polymer Chemistry; Chapman and Hall: London, 1985.
28. Lorenzo, A. T.; Arnal, M.; Albuerne, J.; Muller, A. J. Polym Test 2007, 26, 222.
29. Li, Y.; Tian, G.; Yan, D.; Zhou, E. Polym Int 2001, 50, 677.
30. Hoffman, J. D.; Weeks, J. J. J Res Natl Bur Stand 1962, 66, 13.